

Correlating distributed acoustic sensing (DAS) to natural fracture intensity for the Marcellus Shale

Payam Kavousi*, Timothy Carr, Thomas Wilson, and Shohreh Amini, West Virginia University; Colin Wilson, Mandy Thomas, Keith MacPhail, Schlumberger; Dustin Crandall, US Department of Energy/National Energy Technology Laboratory; BJ Carney, Ian Costello, and Jay Hewitt, Northeast Natural Energy LLC.

Summary

Distributed acoustic sensing (DAS) technology also known as distributed vibration sensing (DVS) uses optical fibers to measure the dynamic strain at all points along the fiber (Parker et al, 2014). The DAS senses the vibration in the local environment around the fiber and provides a measure of the relative strain of the optical fiber. This remote sensing technique has provided unparalleled acoustic sampling from the subsurface during hydraulic fracturing of the horizontal MIP-3H well drilled in Marcellus Shale near Morgantown, WV. We will show that the energy of the extracted phase of DAS data (hDVS) has a strong negative correlation with natural fracture intensity P32. The hydrofracking stages with lower P32 show a higher DAS phase energy and vice versa. In addition, we will evaluate the correlation between DAS phase energy, microseismic energy, and injection energy during the hydrofracking in MIP-3H. DAS phase energy is linearly correlated with injection energy. The calculated microseismic energies, which are less than 0.1% of the injection energies, do not show a significant correlation with either DAS phase energy or injection energy. The negative correlation between P32 and either DAS phase energy or injection energy suggests less vibration in zones that are more naturally fractured. Numerous observed fractures from wireline image logs are resistive (healed), and appear to significantly control the hydrofracking efficiency in MIP-3H.

Introduction

DAS technology is based on the Optical Time Domain Reflectometry (OTDR). A laser pulse travels inside the fiber and will be scattered back encountering natural imperfection in the fiber (Dickenson et al. 2016) (Figure 1). The recorded backscatter contains information of local axial strain along the fiber (Parker et al, 2014). Arrival times of the sent laser pulses are used by DAS signal processing unit to determine the location of the backscatter origin along the fiber. In addition, the Rayleigh peak phase in the backscatter is sensitive to the dynamic strain of the fiber and hence the vibration in the local environment around the fiber. The phase of the Rayleigh peak can be calculated using heterodyne phase detection method (Permeneva, 2014). Dynamic strain of the fiber is linearly proportional to the phase of the Rayleigh peak (Dickenson et al. 2016). The calculated location and the relative strain

provide a vibration profile along the fiber. In this paper we use the processed extracted phase data also known as heterodyne distributed vibration sensing (hDVS). hDVS data is in SEGY format and is recorded during the hydrofracking for each stage. A Matlab script is written to visualize the data and also calculate the energy attribute of the phase data (Figure 2). In addition, microseismic events are recorded for MIP-3H from Stage 07 to the last Stage 28, which is the closest to the heel of the well (Figure 3).

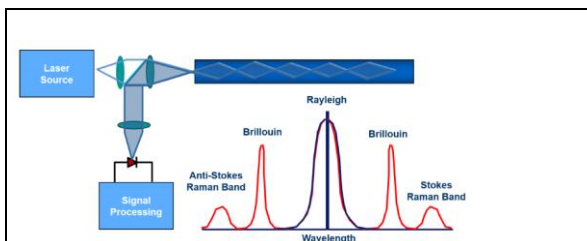


Figure 1: Principle of Optical Time Domain Reflectometry. The original pulse (blue) is sent from the laser source and scattered back to the signal processing unit as the red signal. Courtesy of Dickenson et al., 2016.

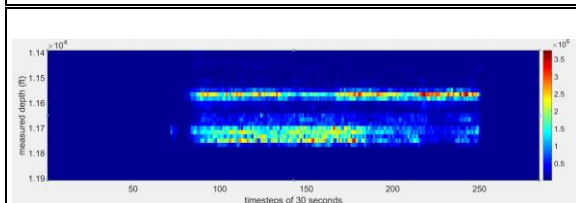


Figure 2: The hDVS data for Stage 10 in MIP-3H well. The data reveals limited to no vibration of the fiber between 11,600 to 11,650 feet corresponding to the perforation clusters 3 and 4.

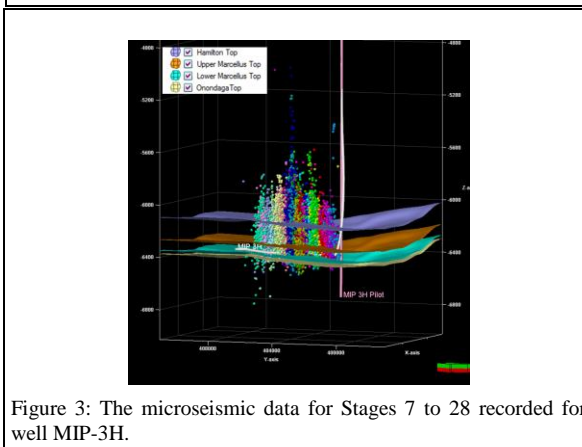


Figure 3: The microseismic data for Stages 7 to 28 recorded for well MIP-3H.

Correlating distributed acoustic sensing (DAS) to natural fracture intensity

The other sources of the data that are used in this paper include treatment pressure, rate, elapsed time during the hydrofracking, and natural fracture intensity (P32) interpreted from wireline image logs.

We show that there is a negative linear correlation between P32 and hDVS energy: stages with lower P32 have substantially higher hDVS energy attribute. The reason might be the less tensile strength of the Marcellus Shale in highly fractured zones along the well path.

We will also show that hDVS energy is linearly correlated with the injection energy during hydrofracking. Finally, microseismic energy is also compared with the injection energy and hDVS energy; no meaningful correlation has been obtained.

MIP-3H completion

Shale reservoir heterogeneity presents a challenge for an efficient hydraulic fracture stimulation. Chorn et al., (2014) studied production performance for 100 wells drilled in the Barnett Shale by an operator; although the drilling and stimulation design were kept constant, a significant production variability was observed. The geometrical completion has been a common method in development of unconventional plays (Anifowoshe et al, 2016). In the geometrical completion the heterogeneity along the lateral is not accounted for. Cipolla et al., (2011) implemented a statistical analysis on 100 production logs from geometrically completed horizontal wells; only 60% of the perforation clusters were contributing to production.

Enhanced engineered completion design for several stages is tested in MIP-3H well. Various geomechanical data acquired by well logging were used to optimize the stage length, cluster spacing and treatment parameters. Stages were strategically placed in segments with similar gamma ray, minimum horizontal stress, and natural fracture intensity (Anifowoshe et al, 2016) (Figure 4). A limited entry approach was undertaken by decreasing the number of shots per clusters to enhance stimulation efficiency (Anifowoshe et al, 2016).

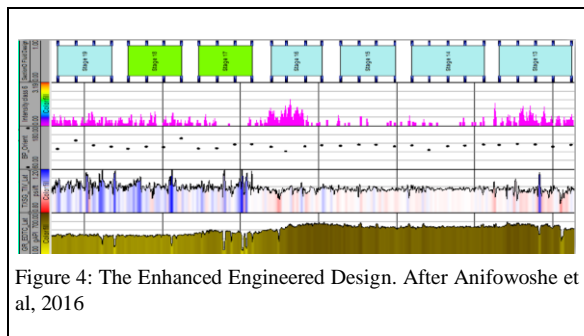


Figure 4: The Enhanced Engineered Design. After Anifowoshe et al, 2016

The engineering stages are considered for further analysis in this paper because of the attempt to group relatively similar gamma ray, minimum horizontal stress, and natural fracture intensity within each stage. Each stage has 4 or 5 clusters of 2ft length, at 4 shots per foot.

Figure 5 shows hDVS data for a geometric stage versus an enhanced engineered stage. Stage 18 shows more uniform vibration along the fiber than Stage 08.

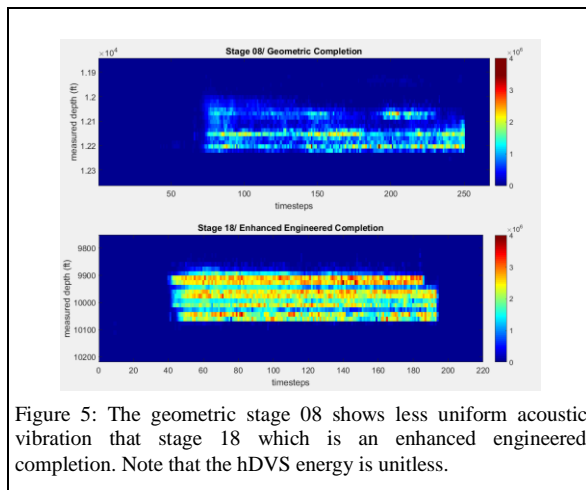


Figure 5: The geometric stage 08 shows less uniform acoustic vibration that stage 18 which is an enhanced engineered completion. Note that the hDVS energy is unitless.

hDVS data structure

hDVS data is recorded along the 28 Stages in the MIP-3H. We will first review the structure of the hDVS data and then discuss the energy attribute analysis for the data. hDVS data represent the phase attribute that is recorded along the length of optical fiber attached to the casing. Phase is linearly proportional to the axial strain along the fiber. hDVS data are in SEG Y format and the location of the vibration in the fiber is recorded in 240 byte trace headers. For every 30 seconds during hydrofracking, there is a SEG Y file that has 493 traces: each trace has 60,000 samples which corresponds to 500 millisecond sampling rate. The 493 traces cover around 8236 ft.; this corresponds to a spatial sample rate along the fiber in MIP-3H lateral of 16.74 ft. The number of the SEG Y files in each stage vary from 200 to 900 files depending on the fracking duration (one SEG Y file every 30 second).

Energy attribute for the hDVS data

We evaluated the hDVS SEG Y files of enhanced engineered completed stages. The energy attribute is calculated on each of the 493 traces for every 30 seconds during the hydraulic fracture stimulation. The energy attribute (Figure 2 and 5) at each time step is calculated as:

Correlating distributed acoustic sensing (DAS) to natural fracture intensity

$$E_i = \sum_{j=1}^{60,000} x(j)^2 \quad i = 1 \dots 493$$

Where $x(j)$ is sample j from 60,000 samples in trace i . Thus there are 493 energy values calculated for every time step of 30 seconds during the fracture stimulation. Then, we calculate the total hDVS energy by stacking the calculated energy for each trace during the fracture stimulation (i.e. stacking of the calculated energies for a location on the fiber for fracture stimulation duration). We calculated the total energy within each stage. For example the total hDVS energy for Stage 10 is only calculated by stacking energy of the traces 357 to 367 ($i=357 \dots 367$).

The energy attribute provides a visual inspection tool on the effectiveness of the stimulation. Figure 2 shows that there are limited to no vibration within a measured depth of 11,600 to 11,650 ft during the fracture stimulation of Stage 10. These interval contain perforation clusters number 3 and 4 of Stage 10.

Energy attribute for the microseismic data

We calculated energy of the microseismic events (E_s) in Joule using the modified Kanamori equation (1977):

$$\log_{10} E_s = 1.5M_0 + 4.8$$

Where M_0 is the magnitude of microseismic events. The calculated energy has an average of 56,771 joule and a standard deviation of 45,622 joule for stages 7 to 28.

Energy attribute for the treatment data

The pumping data is available for each stage during the well treatment. Surface treatment pressure, injection rate, and pumping time provide an approximate of the injection energy as:

$$IE = \int_{t_1}^{t_2} PQ dt$$

The injection energy is estimated using the average values of treatment pressure, treatment rate and the duration of the fracture stage (Boroumand and Eaton, 2012) as:

$$IE = \overline{P(t)} \times \overline{Q(t)} \times \Delta t$$

The average of the injection energy is around 92.4×10^6 kilojoules. A comparison between the microseismic energy and injection energy reveals that the energy associated with the recorded microseismic activities are less than 0.01% of the total injected energy (Table 1). Boroumand and Eaton (2012) showed that microseismic energy is less than 1% of injection energy for 4 wells in an unconventional shale gas.

Stage#	Microseismic Energy (j)	Injection Energy (j)	Mic/Inj ratio%
13	2.74E+04	9.08E+10	3.02E-05
14	4.74E+04	1.03E+11	4.60E-05
15	6.09E+04	8.78E+10	6.94E-05
16	3.28E+04	7.00E+10	4.68E-05
17	3.04E+04	7.89E+10	3.85E-05
18	9.30E+04	8.03E+10	1.16E-04
19	1.00E+05	9.06E+10	1.11E-04

Table 1: Calculated microseismic energy and injection energy in joule for the enhanced engineered stages. Microseismic/injection energy ratio is also shown in percentage.

Fracture intensity attribute

The P32 fracture intensity is calculated using the wireline image logs. Pre-existing natural fractures appear to affect the stimulation process. Gale et al., (2008) analyzed natural fractures of Barnett Shale core from Pecos County, Texas. The tensile testing on the cores showed failure along fractures even though fractures are sealed. They proposed that the Barnett Shale in the Fort Worth Basin has sealed natural fractures that affect hydraulic fracture propagation. This could be a result of reactivation of natural fractures and hence hydraulic fracture propagation at natural fracture tips. The computerized tomography (CT) of the vertical core from the MIP-3H pilot hole shows several natural fractures in Marcellus Shale that are mineral filled (Figure 6). More than 1500 resistive (healed) fractures are documented from the wireline image logs in the MIP-3H.

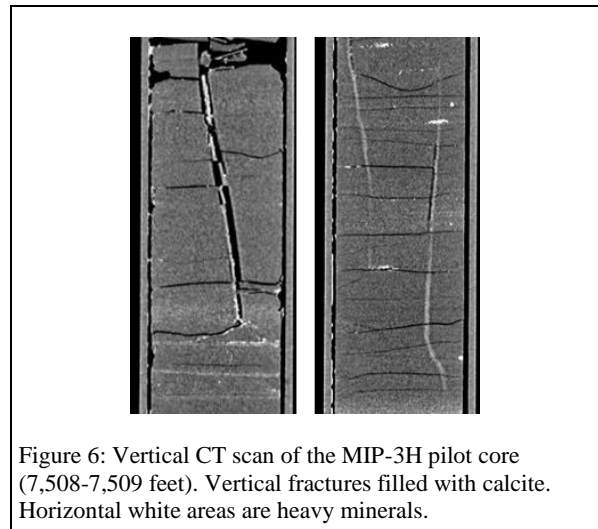


Figure 6: Vertical CT scan of the MIP-3H pilot core (7,508-7,509 feet). Vertical fractures filled with calcite. Horizontal white areas are heavy minerals.

Correlating distributed acoustic sensing (DAS) to natural fracture intensity

Discussion

For the MIP-3H the energy attribute was calculated from the hDVS data, microseismic data, and treatment data. We then compare these attributes to unravel correlation between attributes. Our analysis shows that there is strong negative correlation between hDVS energy and P32 fracture intensity ($R = -0.88$, $p\text{-value} = 0.0191$) for the enhanced engineered completion stages (Figure 7). This negative correlation suggest that stages with more natural fractures are vibrating less than stages with low P32, and might show the role of the strong effect of pre-existing natural fractures in fracture stimulation efficiency. Stages with lower P32 required more energy to develop hydraulic fractures. In contrast, stages with high P32 are easier to break and hence a lower hDVS energy is observed. Although the majority of the fractures observed in MIP-3H are healed fractures, they enhance the hydraulic fracturing in the MIP-3H stages.

Our correlation analysis reveals that the microseismic energy is not correlated with either injection energy or hDVS energy. Wilson et al, (2016) calculated an average distance of 190ft. between center of the radiated microseismic energy and the MIP-3H wellbore. Thus, the microseismic energy is distributed through the Hamilton Group and not localized in the vicinity of the perforations, while hDVS measures the local vibrations around the fiber, and fracture stimulation in the Lower Marcellus Shale.

We also showed that hDVS energy is linearly correlated with the injection energy. However, the exact analytical equation that relates hDVS energy to injection energy per stage has not been established and requires more accurate

modeling of the fluid energy in the downhole stages accounting for energy loss during hydraulic fracture stimulation.

Conclusions

- 1- hDVS energy attribute is correlated with the approximate injection energy for MIP-3H enhanced engineered stages.
- 2- hDVS energy shows a negative correlation with the natural fracture intensity per stage (P32). It suggest that stages with higher pre-existing natural fractures are easier to break and hence less hDVS vibration along the stage is observed.
- 3- CT scan and wireline image logs show numerous vertical mineral-filled fractures in the Marcellus Shale in the MIP-3H. Our analysis shows that even though the majority of pre-existing fractures are mineral-filled, they might strongly influence the fracture stimulation process.
- 4- Although microseismic events provide valuable clues concerning the extent of hydraulic fractures, they represent less than 0.01% of the total injection energy.
- 5- We observed no significant correlation between microseismic energy and P32, injection energy, and hDVS energy. We suggest that the microseismic is responding to induced stress in the overlying Mahantango Formation an average 190 ft. above the borehole.
- 6- The proposed energy attribute of the hDVS data is shown to be a valuable computed attribute, which can be applied on-site to assess hydraulic fracture stimulation efficiency.

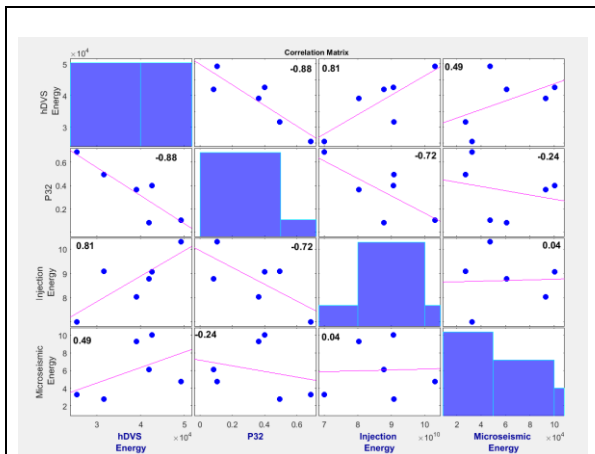


Figure 7: the correlation matrix of variables: Microseismic Energy, Injection Energy, Mean P32, and hDVS Energy. The R value is posted for each pair of variables.

Acknowledgement

This research is funded through the U.S.DOE National Energy Technology Lab part of their Marcellus Shale Energy and Environmental Laboratory (MSEEL) (DOE Award No.: DE-FE0024297).

We also would like to appreciate MathWorks for Matlab software, and Schlumberger for Petrel software.

The authors would like to thank Paul Dickenson from Nuron Technology for helpful discussions about the hDVS data.

EDITED REFERENCES

Note: This reference list is a copyedited version of the reference list submitted by the author. Reference lists for the 2017 SEG Technical Program Expanded Abstracts have been copyedited so that references provided with the online metadata for each paper will achieve a high degree of linking to cited sources that appear on the Web.

REFERENCES

- Anifowoshe, O., M. Yates, L. Xu, P. Dickenson, J. Akin, B. J. Carney, J. Hewitt, I. Costello, and Z. Arnold, 2016, Improving wellbore stimulation coverage in the marcellus: Integrating lateral measurements with enhanced engineered completion design and fiber optic evaluation: In SPE Eastern Regional Meeting Society of Petroleum Engineers, <https://doi.org/10.2118/184051-MS>.
- Boroumand, N., and D. W. Eaton, 2012, Comparing energy calculations-hydraulic fracturing and microseismic monitoring: 74th Annual International Conference and Exhibition, EAGE, Extended Abstracts, EUROPEC 2012, <https://doi.org/10.3997/2214-4609.20148187>.
- Chorn, L., N. Stegent, and J. Yarus, 2014, Optimizing Lateral Lengths in Horizontal Wells for a Heterogeneous Shale Play: Presented at the SPE/EAGE European Unconventional Resources Conference and Exhibition, <https://doi.org/10.2118/167692-MS>.
- Cipolla, C. L., X. Weng, H. Onda, T. Nadaraja, U. Ganguly, and R. Malpani, 2011, New algorithms and integrated workflow for tight gas and shale completions: Presented at the SPE Annual Technical Conference and Exhibition, SPE, <https://doi.org/10.2118/146872-ms>.
- Dickenson, P., S. Brants-Menard, M. Telsey, A. Stanbridge, C. Wilson, J. Akin, N. Roman, O. Anifowoshe, M. E. Yates, B. J. Carney, and I. Costello, 2016, Real-time interactive remote display of DTS and DAS data for well treatment optimization: Presented at the SPE Intelligent Energy International Conference and Exhibition, SPE, <https://doi.org/10.2118/181065-ms>.
- Gale, J. F., R. M. Reed, S. P. Becker, and W. Ali, 2008, Natural Fractures in the Barnett Shale in the Delaware Basin, Pecos Co. West Texas: Comparison with the Barnett Shale in the Fort Worth Basin.
- Kanamori, H., 1977, The energy release in great earthquakes: *Journal of Geophysical Research*, **82**, no. 20, 2981–2987, <https://doi.org/10.1029/JB082i020p02981>.
- Parker, T., S. Shatalin, and M. Farhadiroushan, 2014, Distributed Acoustic Sensing — A new tool for seismic applications: *First Break*, **32**, 61–69, <https://doi.org/10.3997/1365-2397.2013034>.
- Permeneva, D., 2014, Optical heterodyne detection of phase-shifted signals: M. Sc. Thesis, Rochester Institute of Technology.
- Wilson, T., T. Carr, B. J. Carney, J. Hewitt, I. Costello, E. Jordon, K. MacPhail, N. Uschner, M. Thomas, S. Akin, and O. Magbagbeola, 2016, Microseismic and model stimulation of natural fracture networks in the Marcellus Shale, West Virginia: 86th Annual International Meeting, SEG, Expanded Abstract, 3088–3092, <https://doi.org/10.1190/segam2016-13866107.1>.